Open Journal of Marine Science, 2016, 6, 440-455
Published Online July 2016 in SciRes. http://www.scirp.org/journal/ojms
http://dx.doi.org/10.4236/ojms.2016.63037

Effects of Monsoon Winds and Topographical Features on the Vertical Thermohaline and Biogeochemical Structure in the Gulf of Tadjourah (Djibouti)

Youssouf Moussa Omar[1,2], Laurent Memery[2], Xavier Carton[3], Abdourahman Daher[1], Eric Duvielbourg[2]

[1]Centre d'Etude et de Recherche de Djibouti Route de l'aéroport, Djibouti, Djibouti
[2]Laboratoire des sciences de l'environnement Marin (LEMAR) Institut Universitaire Européen de la Mer (IUEM) Technopole Brest Iroise, Plouzané, France
[3]Université de Bretagne Occidentale (UBO) Laboratoire de physique de l'Océan, Brest, France
Email: xavier.carton@univ-brest.fr

Received 7 March 2016; accepted 25 July 2016; published 28 July 2016

Abstract

The vertical thermohaline and biogeochemical structures of the upper layer (0 - 200 m) were studied in the Gulf of Tadjourah using high-resolution hydrographic data collected in July-August 2013, September 2013 and February 2014. During summer, the superficial layer consisted of the mixed layer (ML) extending to a depth of about 20 - 30 m followed by the thermocline located between 30 and 50 m depth. The ML was thicker in the west and the southeast where the thermal gradient and chlorophyll *a* concentrations were particularly high. During September, this stratification persisted but the ML became warmer and saltier and the thermocline moved slightly deeper. In February, the ML extended to about 120 m, and the thermocline was less pronounced. A comparison of the directly measured currents to the wind induced Ekman current and to geostrophic velocity profiles revealed that the thermohaline and the biogeochemical features in summer were related to the southwest monsoon (SWM). The SWM drives surface water from the Gulf of Tadjourah to the Gulf of Aden and thus induces westward intrusion of the high salinity thermocline water from the Gulf of Aden; this near surface flow mixes surface waters in the extreme west of the Gulf of Tajourah. In contrast, the northeast monsoon (NEM), predominant in winter, brings cold water toward the Gulf of Tadjourah and thickens the ML through convective mixing. Our study shows that the SWM plays a crucial role in the stratification of the water column during summer but bathymetry influences its effects. The bowl-shape of the basin and its elongated slope in the west enhance the upwelling in this area where negative sea surface temperature anomalies and high chlorophyll *a* concentrations were observed.

How to cite this paper: Moussa Omar, Y., Memery, L., Carton, X., Daher, A. and Duvielbourg, E. (2016) Effects of Monsoon Winds and Topographical Features on the Vertical Thermohaline and Biogeochemical Structure in the Gulf of Tadjourah (Djibouti). *Open Journal of Marine Science*, **6**, 440-455. http://dx.doi.org/10.4236/ojms.2016.63037

Keywords

Thermohaline, Biogeochemical Structures, Mixed Layer Depth, Thermocline, Monsoon Wind, Topography

1. Introduction

The Gulf of Tadjourah (GOT hereafter) is located at the western end of the Gulf of Aden and to the southeast of the Bab Al-Mandeb Strait which connects the Red Sea to the Indian Ocean. Extending over about 4500 km^2, this semi-enclosed sea is an extension of the rift of Tadjourah (**Figure 1**) and penetrates deeply into the continent through the Ghoubet El Kharab Bay. Here it is bordered by the Afar Depression, one of the hottest and volcanically most active areas in the world [1] [2].

From both social and economic perspectives, the GOT plays a crucial role as a local fishing area. It is also vital in securing food to coastal communities of the surrounding arid lands of Djibouti. In the context of current concerns regarding the effects of global warming, vulnerable marine habitats and their resources may be detrimentally impacted and therefore, it is essential to establish a fishing policy based on scientific knowledge of the ecosystem and its potential for exploitation. Surprisingly, the oceanographic data are scarce and the area remains poorly studied.

Recently, the main patterns of temporal and spatial variability at the surface in the GOT were identified using satellite historical data on sea surface temperature (SST) from AVHRR MetopA radiometer and a merged product on ocean color from Modis/Meris sensors (Glob Colour/ST-ACRI), [3]. This work showed that SST is well correlated to the net surface heat flux during winter (November-May), while during summer (June-September), neither SST nor chlorophyll *a* (CHL-*a*) concentrations have a significant correlation with the studied atmospheric parameters (wind speed, air temperature and specific humidity). Except for this statistical covariance analysis, the processes governing SST and CHL-*a* concentration patterns in the GOT are poorly understood.

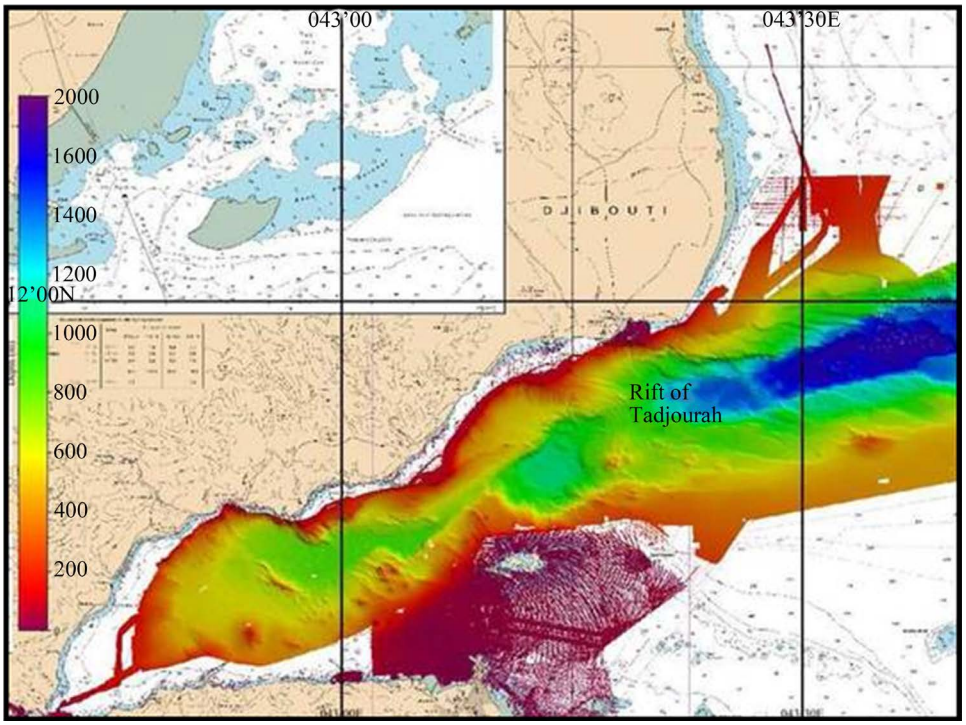

Figure 1. Map of the Gulf of Tadjourah showing bathymetric features. Note the two troughs along the continuation of the Rift of Tadjourah and the wider continental shelf in the southeast of the gulf (purple area).

The limited available data on the water column in the GOT originate exclusively from research vessels passing through Djibouti on their way to study other ocean areas. Thus, during pelagic fish sampling, Myklevoll [4] collected CTD profiles in the east and in the center of the GOT, thereby locating the thermocline at 85 m and 60 m depth, respectively. Twenty years later, some vertical profiles containing data on temperature, salinity and dissolved oxygen (DO) were obtained during the first Red Sea Outflow Experiment (RedSOX-1, see Bower and Fratantoni, 2002) in the northeastern part of the GOT. These data indicated a thermocline and a pycnocline at about 100 m depth. In addition, descriptive ecological studies [5]-[7] reported the presence of a seasonal thermocline. Unfortunately, all these studies were sporadic, localized in space or focused on other subjects. They did not provide a clear vertical structure of the water column, as it evolves throughout the year.

The questions addressed in this paper are: 1) How is the water column structured during summer time and how does it evolve throughout the year? 2) How does the vertical structure contribute to the observed variability of SST and CHL-*a*? These questions are dealt with using newly collected data in the GOT. These successively collected data as well as new analysis methods [8] [9] used in this study are presented in Section 2. In Section 3, the vertical thermohaline and biogeochemical structures of the upper layer (0 - 200 m) during summer and their temporal evolution in September and February are analyzed. Finally, discussion and conclusions are presented in Section 4.

2. Data and Methodology

2.1. *In Situ* Measurements and Pre-Processing

The hydrologic data were collected successively during three particular periods: July-August (summer), September 2013 (transitional period), and February 2014 (winter) at eight stations in the GOT (see **Figure 2** for geographic location of the sampling stations). Data on temperature, pressure, salinity, fluorescence (CHL-*a*), DO and dissolved organic matter (DOM) were obtained using a multiparameter sensor (YSI EXO2). For direct

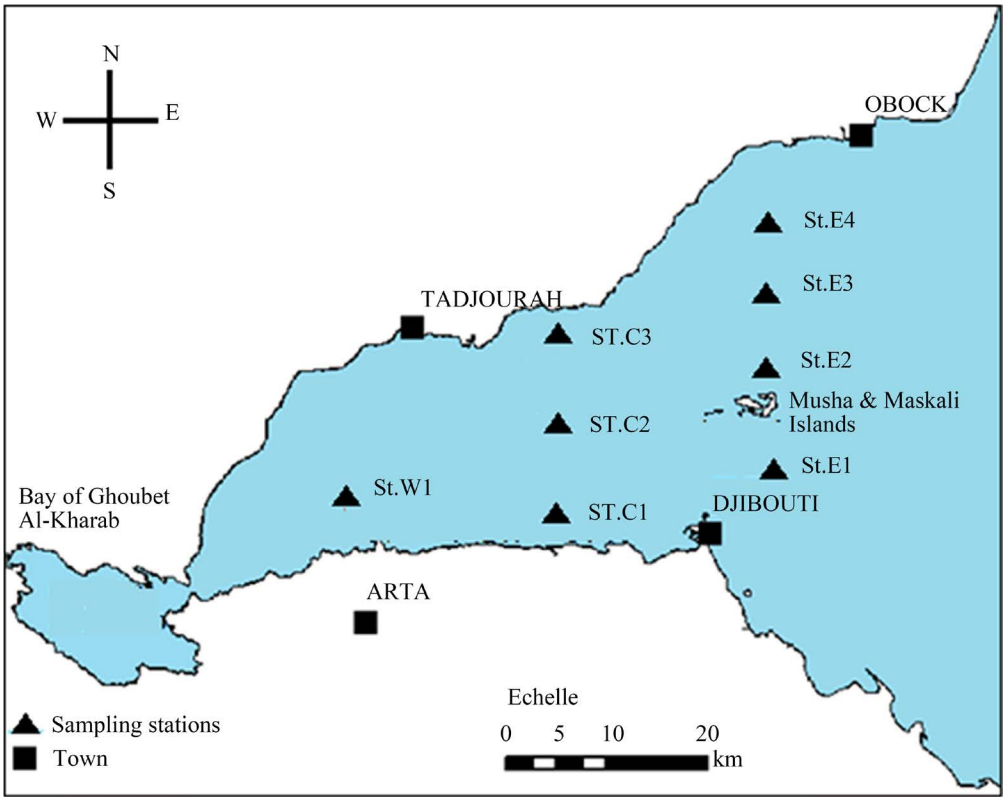

Figure 2. Schematic map of the Gulf of Tadjourah showing the location of the eight sampling stations. The stations located at the center (C1, C2 and C3) and in the east (E1, E2, E3 and E4) are aligned with the longitudes 43˚00'E and 43˚10'E, respectively.

current measurements, a Seaguard sensor, with an ADCP (Acoustic Doppler Current Profiler) was used. At each station, the two instruments were used simultaneously and data were recorded both during descent and ascent of the probes. Two or three immersions were carried out at each station. Thus, at least four vertical profiles were obtained for each parameter and at each station. For two probes, data specifications are presented in **Table 1**.

To assess the quality of the data, the standard deviation was computed from the total number of profiles. Thus, values exceeding more than three standard deviations (3σ) were systematically removed. Each profile was subsequently checked for an inversion in depth which may have been generated by boat instability at the sea surface. All the data were smoothed by 5-points moving average and interpolated between the surface and 200 m.

2.2. Methodology

2.2.1. Vertical Profile Data Analysis

The vertical structure of the upper layer (0 - 200 m) was studied by means of data profile analysis. Firstly, the thermal vertical structure was examined using temperature gradient profile analysis. In contrast to the commonly used gradient criterion based on a predetermined threshold value [10], here the mean gradient value ($\overline{Gr}$) was used, as computed from the profile data between the surface and a certain depth (Z_l). This depth is estimated from the theoretical depth of the thermocline (Z_{th}) as shown below:

$T_{th} = \dfrac{T_{\max} + T_{\min}}{2}$; $T_{\max}$; $T_{\min}$: the maximum and the minimum of the temperature profile

$Z_{th} = Z\left(T_{th}\right)$; the corresponding theoretical depth of the thermocline

$$Z_l = 2 \times Z_{th}; \tag{1}$$

Thus, from the surface downward, the part of the profile where the temperature gradient remains below $\overline{Gr}$ is considered the mixed layer. The thermocline was defined as the area where the temperature gradient exceeds $\overline{Gr}$.

The Mean Gradient Method (MGM) was then compared to two objective methods for determining mixed layer depth from the profile data: the Maximum Angle Method (MAM) and the Curvature Method (CM). The MAM is based on an angle between two successive vectors along the profile (**Figure 3**). This method is implemented in three steps: 1) fitting the profile data with a first vector (pointing downward) from a selected near-surface depth to a deeper level and a second vector (pointing downward) from that second depth to a deeper level, 2) identifying the angle (varying with depth) between the two vectors and 3) finding the depth (*i.e.*, the mixed layer depth) with the maximum angle between the two vectors. The MAM is sensitive to the number of points (n) vertically used for vector 1 and vector 2. Here we used n = 7 for which RMSE between MAM and MGM was minimum. The CM is based on the second-order derivative computed at each depth Z_k as shown in Equation (2) below. At the curvature point of the profile, the second-order derivative has a minimum value which corresponds to the mixed layer depth (MLD). More details on these objective methods can be found in [8] [9] [11].

$$\frac{\partial^2 T}{\partial z^2} = \frac{1}{\left(z_{k+1} - z_k\right)}\left(\frac{T_{k+1} - T_k}{z_{k+1} - z_k} - \frac{T_k - T_{k-1}}{z_k - z_{k-1}}\right) \tag{2}$$

Table 1. Data specification for measured parameters.

Measured parameter	Range	Accuracy	Resolution
Temperature (˚C)	−5˚C to 35˚C	±0.01˚C	0.001˚C
Conductivity (mS/cm)	0 - 100 mS/cm	±0.001 mS/cm	0.0001 - 0.01 mS/cm
Depth (m)	0 - 200 m	±0.003 - 0.004 m	0.001 m
Dissolved Oxygen (mg/l)		±0.1 mg/l	0.01 mg/l
Chlorophyll *a* concentration	0 - 280 µg/l	-	0.01 µg/l
Current velocity (m/s)	0 - 300 m	1%	0.01 m/s
Current direction (˚)	0 - 300 m	±5˚	0.01˚

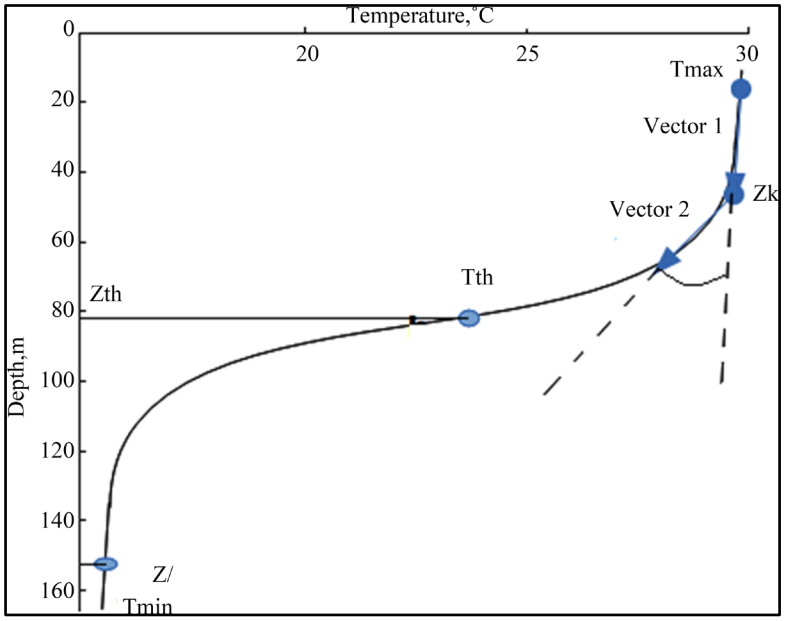

Figure 3. Diagram indicating maximum angle method (vector 1 and vector 2) and mean gradient method (T_{max}, T_{min}, T_{th}, Z_{th} and Z_l).

Subsequently, the vertical variation of salinity, CHL-*a* concentration (fluorescence), DO, currents and nutrients were studied exclusively using the individual profile data and cross-section analysis.

2.2.2. Surface wind Induced Current (Ekman Derived)

The Ekman surface current was estimated from wind stress gridded data at 0.125˚ × 0.125˚ resolution (source). At each grid point, the zonal and meridian components were computed using Equations (3) and (4) (see [12]).

$$u = \frac{\tau_x}{\rho_0\sqrt{Az \times f}}\sin(4) + \frac{\tau_y}{\rho_0\sqrt{Az \times f}}\cos(4) \tag{3}$$

$$v = \frac{-\tau_x}{\rho_0\sqrt{Az \times f}}\cos(4) + \frac{\tau_y}{\rho_0\sqrt{Az \times f}}\sin(4) \tag{4}$$

Az: coefficient of vertical viscosity; ρ_0: density of the surface water; *f*: Coriolis parameter

2.2.3. Geostrophic Current Velocity

At each station, the specific volume anomaly ($\alpha = 1/\rho$) was computed from the sea surface to a depth of 200 m, as a function of temperature, salinity and pressure, using seawater state equations. Then, the differences of geopotential between two stations were integrated between reference pressure P_0 and pressure *P* at depth *z*.

$$\Phi = \int_{P_0}^{P} \alpha(P,S,T) \tag{5}$$

Geostrophic current between stations B and A, separated by distance *L*, is given by :

$$U = -\frac{1}{fL}\{(\Phi b) - (\Phi a)\} \tag{6}$$

3. Results

3.1. Vertical Structure in Summer

Figure 4 shows vertical profiles of temperature, density, salinity, DO, DOM for the summer period (July-August 2013). In the following sections the thermohaline and the biogeochemical structures are described separately.

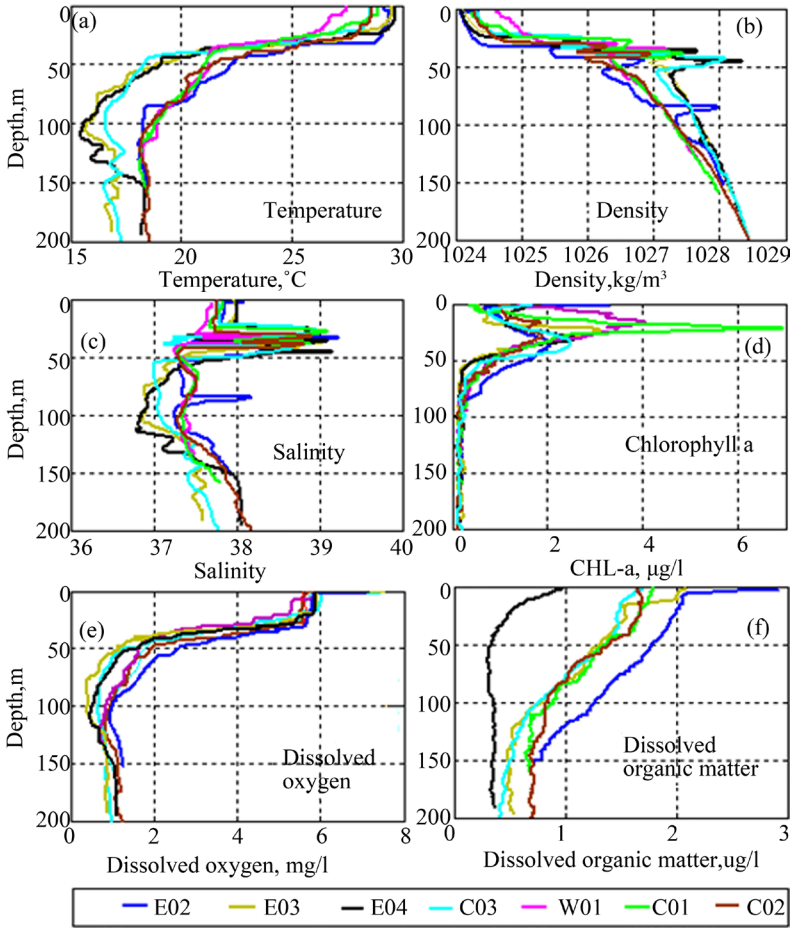

Figure 4. Vertical profiles of temperature, density, salinity, dissolved oxygen and dissolved organic matter at 8 stations in the Gulf of Tadjourah.

The relation between the two will be examined thereafter.

3.1.1. Thermohaline Structures

1) Temperature

From **Figure 4(a)**, five zones can be distinguished in the vertical temperature profiles for all stations. Near the surface to a certain depth (zone 1), temperatures remain quasi-uniform. Then, it drops rapidly by about 0.5˚C/m between approximately 30 m and 50 m depth (zone 2). In this layer the gradient is much higher than the mean gradient ($\overline{Gr}$). Note also that the thickness of zone 1 (isothermal layer), as well as zone 2 (high thermal gradient), varies between stations. Below zone 2, temperature decreases slowly until 100 m depth (zone 3), then becomes constant below this depth (zone 4). Note, in this zone there is an inversion of the temperature gradient at stations E3, E4 and C3. The density profiles show an identical vertical structure, except for some inversion in zone 2.

The first two zones, which can be distinguished clearly due to their thermal gradient, were identified as the ocean mixed layer and the thermocline. In order to characterize the mixed layer well and to quantify its thickness (MLD), the MGM and the above described two objective methods (MAM and CM) were applied to temperature profiles. **Table 2** shows the isothermal layer depth (HT) and the upper and lower limits of the thermocline. MAM and CM show similar results for HT while the MGM indicates slightly different values for H_T. All three methods highlight spatial variation of the MLD.

2) Salinity

As with temperature, salinity remains quasi-uniform in the first 20 meters. In contrast, the salinity profiles indicate strong fluctuations of the maxima and minima particularly between 30 and 50 m depth where the thermocline

was identified. The observed inversions of density in the pycnocline appear to be due to these variations in salinity rather than temperature. With the exception of station E2, salinity decreases slowly below the pycnocline and then increases below 100 m as observed for temperature (**Figure 4(c)**). However, note that at stations E3, E4 and C3 temperature and salinity are low below 50 m, compared to other stations.

3.1.2. Biogeochemical Structure

At all stations, CHL-*a* is low between the surface and about 20 m depth below which it increases and reaches maximum values between 20 and 35 m. These maxima are highest at stations C1 and W1 (6.96 and 4.13 mg/l, respectively, **Table 3**) and are found at a surprisingly shallow depth. Below 50 m depth, CHL-*a* is lower and remains close to zero at 100 - 200 m depth at all stations. The DOM is high at the surface but decreases with depth. The DO shows similar evolution to the temperature profiles.

The concentrations of nutrients (phosphate, ammonium, nitrite, and silicate) were measured every 10 m from the surface to 160 m depth at stations W1, C1, C2 and E2 during July-August 2013. The vertical distribution of each element is illustrated in **Figure 5**. High concentrations were observed between 40 and 60 m for nitrite and phosphate, at 100 m for silicates and near the surface for ammonium. The maximum concentration of phosphate was reached at 60 m at station C1.

3.2. Temporal Evolution of Thermohaline and Biogeochemical Structure

In order to examine how the water column structure described in section 3.1 evolves over time, the vertical profiles and sections during July-August 2013 were compared to those obtained during September and February 2014. As can be seen in **Figure 6** from the individual profiles at station E2, the thermal structure shows notable

Table 2. Mixed layer depth (H_T = MLD) as estimated from curvature method, maximum angle method and mean gradient method. The upper and lower limits (*Zup* and *Zlow*) and the maximum gradient depth (MaxGrD) of the thermocline are estimated from the thermal gradient profile.

STATIONS	Mean gradient	H_T (m)			THERMOCLINE		
	(˚C/m)	CM	MAM	MGM	Zup	MaxGrD	*Zlow*
E01	−0.04	5.5	5.6	5.67	-	-	-
E02	−0.13	29.7	29.6	29.65	30.9	31.80	44.20
E03	−0.18	15.62	16.3	15.39	31.3	34.30	40.50
E04	−0.17	24.8	21.0	20.57	24.0	32.60	44.40
C01	−0.12	10.0	6.0	6.86	22.7	38	43.10
C02	−0.11	25.1	25.8	25.10	28.6	41	47.90
C03	−0.16	16.6	23.3	16.30	24.10	33.7	38.70
W01	−0.10	13.7	3.9	11.60	28.24	32	35.20

Table 3. Deep Chlorophyll Maximum (DCM) and their depth at 8 stations in the Gulf of Tadjourah.

Stations	DCM (µg/l)	Depth (m)
E2	2.06	35.67
E3	3.1	24.03
E4	2.59	30.8
C2	1.89	28.34
C3	2.48	34.94
C1	6.96	21.57
W1	4.13	18.33

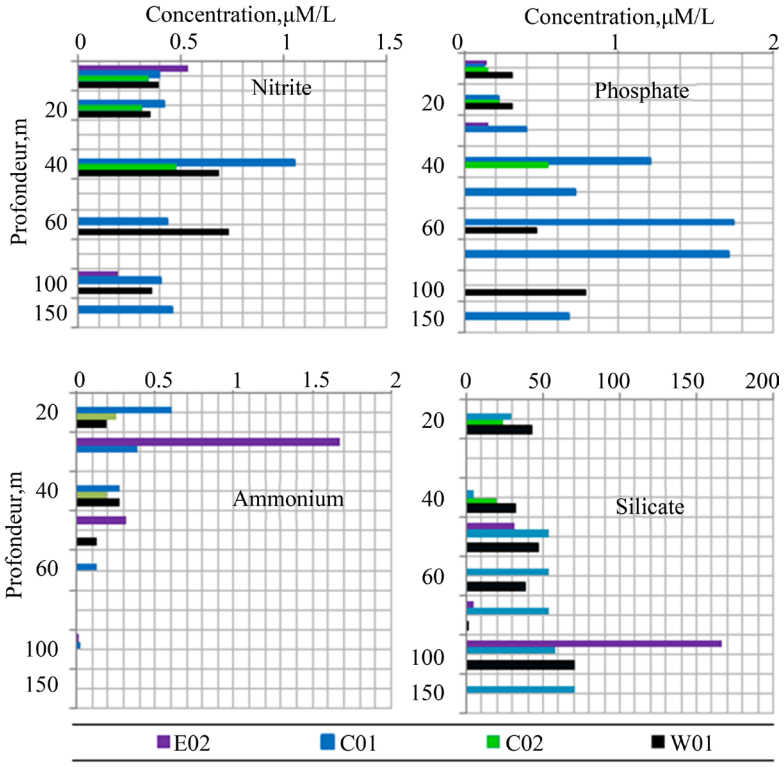

Figure 5. Vertical distribution of nutrients (0 - 160 m) during July-August 2013.

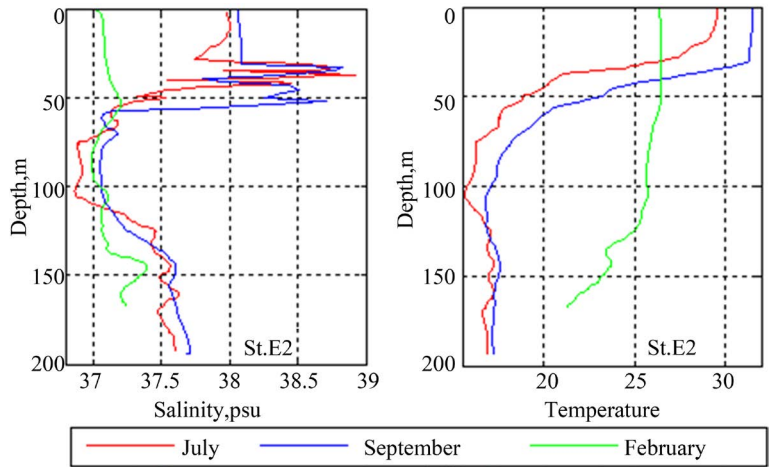

Figure 6. Salinity profiles (left) and temperature profiles (right) at station E2 during July-August (red), September (blue) and February (green).

differences between the three periods. From July-August to September (red and blue curves, respectively), temperature has increased in the mixed layer and the thermocline has deepened by a few meters. This slight difference continues down to about 120 m depth. By February (green), temperature has decreased by about 5˚C and the vertical structure has completely changed. The temperature is homogeneous from the surface down to 120 m and the thermocline has disappeared. In terms of salinity, the mixed layer becomes saltier in September. However, in February salinity is greatly reduced.

The East-West sections of temperature and salinity give more detail on spatial and temporal evolution of the vertical thermohaline structure.

As illustrated in **Figure 7**, temperatures are more or less heterogeneous from the surface to 30 m depth during

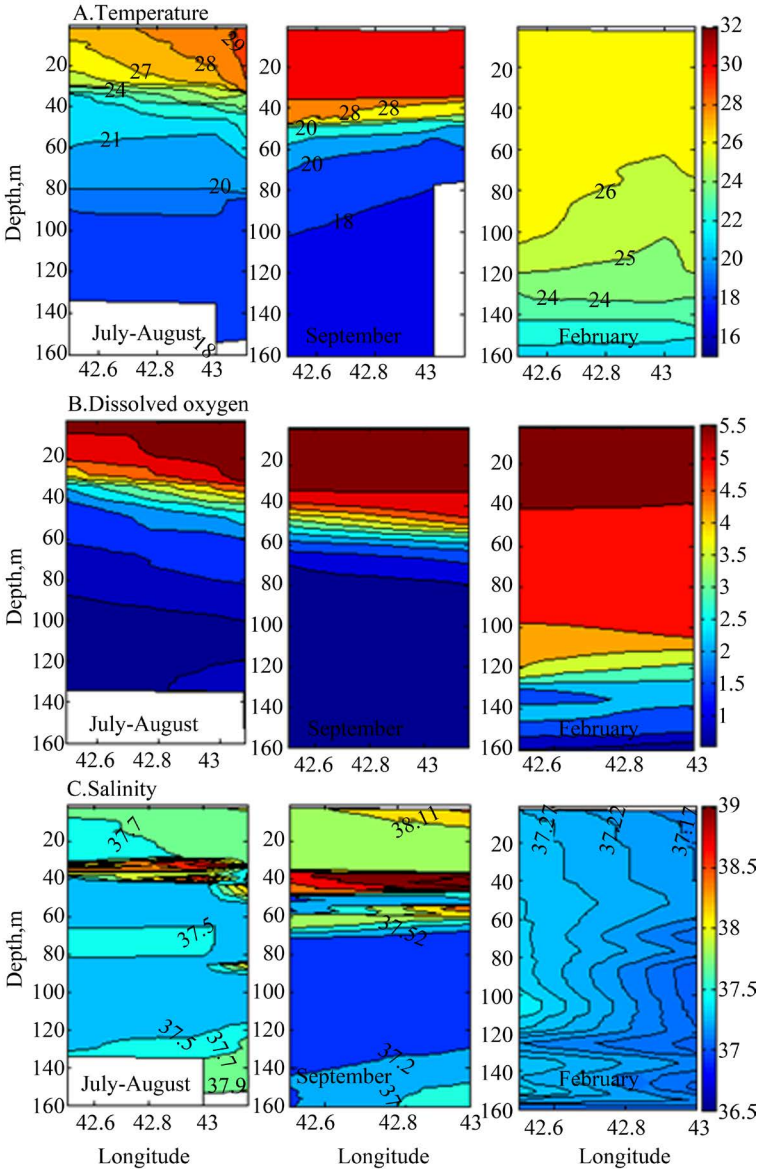

Figure 7. East-west sections of temperature (top panels) and dissolved oxygen (middle panels) and salinity (lower panels) during July-August (left), September (middle) and February (right).

July-August, all isotherms are declined from the west to the east, indicating upwelling in the west. Between 30 m and 60 m, isotherms 22˚C - 24˚C-are tightening, which corresponds to the above identified thermocline from the individual temperature profiles. In September, the upper layer is more stratified. The mixed layer is warmer (T > 30˚C), more homogeneous and extends to about 40 m depth. The thermocline is well pronounced and is located between 34 and 60 m depth. The salinity layer in the thermocline thickens and extends deeper to about 75 m depth. In February, the thermal structure is notably different. The temperature (26˚C - 26.5˚C) and salinity (37.2 psu) are lower and more homogeneous from surface to 120 m. A slight salinity gradient can be observed from the east to the west. The E-W section of DO show similar temporal and spatial evolution to those of temperature.

The biogeochemical structure also shows noticeable seasonal variation. During July-August the DCM is about 20 m beneath the surface and located in the western parts of the Gulf. In September, the higher chlorophyll patch extends eastwards but becomes more narrow and deeper (**Figure 8**). Below 40 m depth, CHL-*a* remains less than 1 µg/l. In contrast, during February, CHL-*a* is low in the entire upper layer from surface to 160 m and does

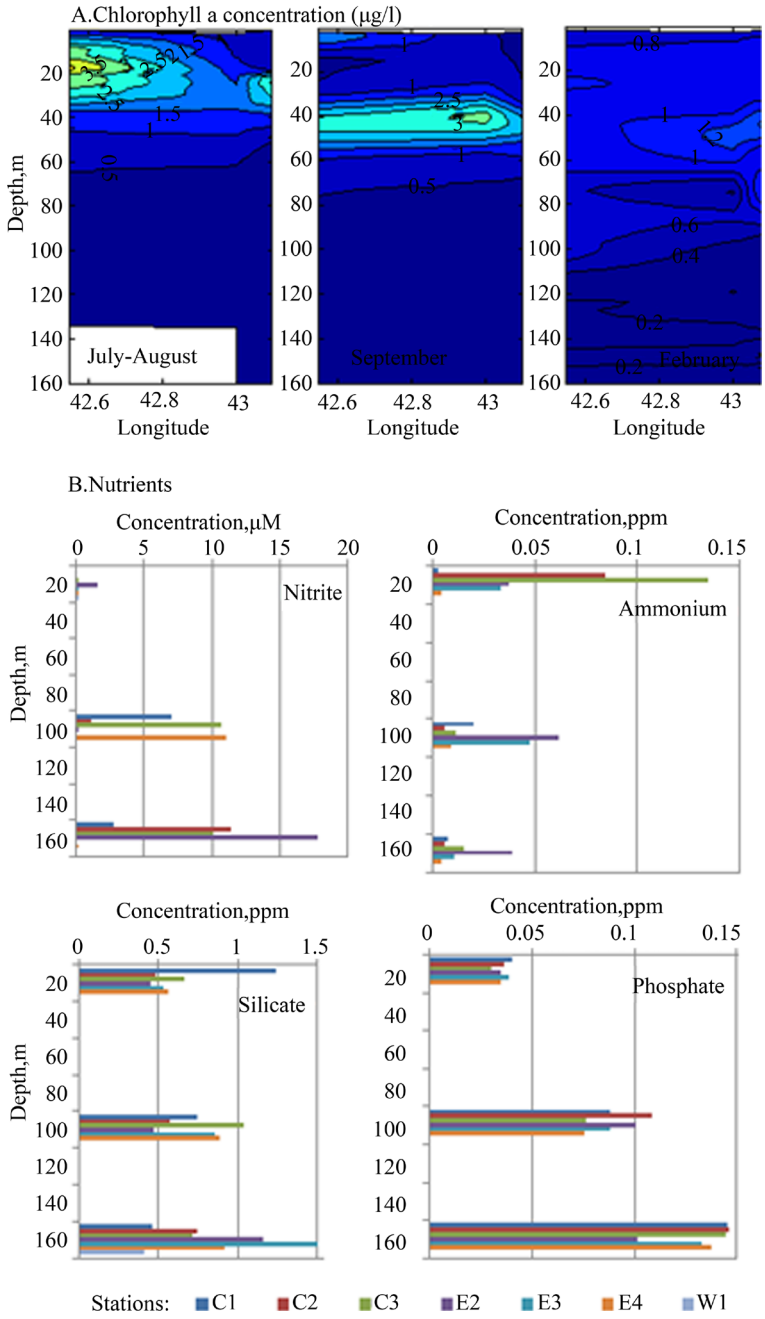

Figure 8. Above: Evolution of vertical structure of chlorophyll-*a* concentration (µg/l) in the Gulf of Tadjourah during July-August (left), September (middle) and February (right). Below: Nutrient concentrations at 8 stations at 3 different depths in February.

not exceed 1.2 µg/l. The vertical structure shows for all nutrients, except ammonium, that the high concentrations are located at a deeper level than in summer (**Figure 8**).

3.2.1. Processes Controlling Thermohaline and Biogeochemical Structure

During July-August 2013, currents were measured in the east (St. E2), south (St. C1) and west (St. W1) of the GOT. **Figure 9** shows vertical profiles of current direction (above) and zonal and meridional components of current velocity (below) between the surface and 200 m depth. As the current vectors show, the direction is

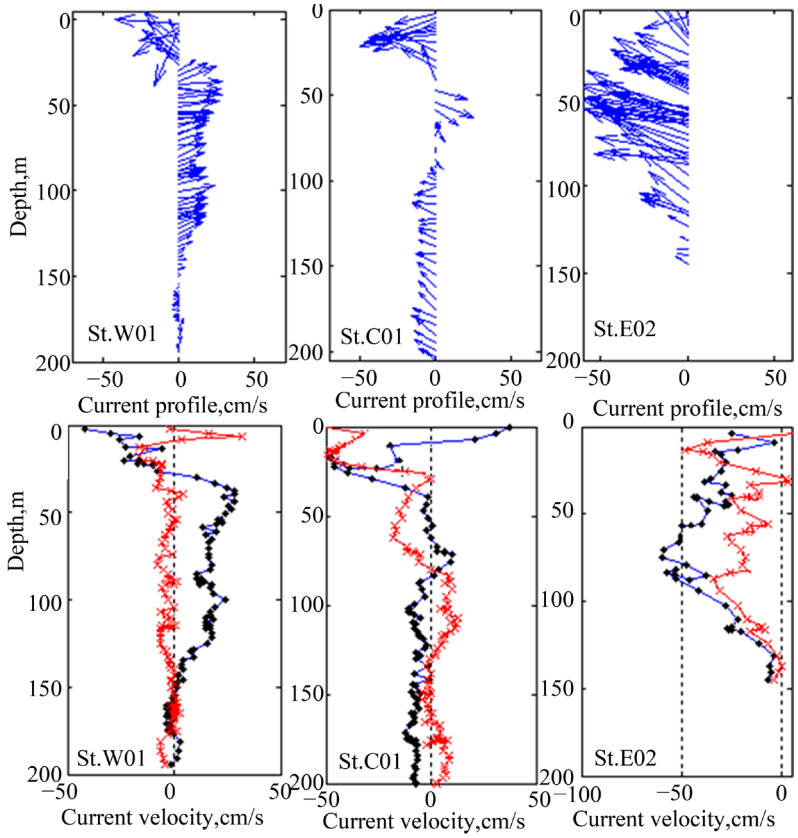

Figure 9. Directly measured current profiles at stations W1, C1 and E2 during July-August 2013. Top panels: current direction, lower panels: zonal component (blue) and meridional component (red).

westward at station E2. The maximum velocity (50 cm/s) is reached at about 50 m depth and the minimum at 150 m. In the south (St. C1), the current has the same direction except at 50 - 60 m where it reverses. In the west (St. W1), the current is westward within the first 30 m and eastward below this depth. Comparatively, the current velocity is high at the eastern station and lower at the western and southern stations.

1) Influences of wind induced surface current (Ekman derived current)

The monthly mean of Ekman derived current vectors superimposed to wind stress field were calculated for the area 11˚N - 14˚N and 42˚E - 44˚E (**Appendix 1**). In the GOT (framed area) currents are toward the South-East from July to September and in the opposite direction (North-West) from October to June. In order to examine the spatial variation of the wind stress inside the gulf, wind stress field from SeaWind sensor gridded data at 0.25˚ × 0.25˚ were linearly interpolated to 0.125˚ × 0.125˚. This revealed that the wind stress is strong at the extreme west of the gulf during July and decreases in August (**Figure 10**).

3.2.2. Geostrophic Current

The zonal and meridional components of the geostrophic velocity were estimated from the hydrographic data collected at stations E2 and E4 during July-August. A vertical profile of the geostrophic current was computed at each depth relative to the reference level fixed at 150 m using Equation (4) with L = 10,000 m (distance between two stations) and the Coriolis parameter at latitude 11˚40: $f = 2.88 \times 10^{-5}\ s^{-1}$. The directly measured current at this level is lower or close to zero (see **Figure 6**). **Figure 11** shows zonal and meridional components during July-August. The two components remain negative from the surface to 150 m depth where it vanishes. This is consistent with the directly measured current during July-August (see **Figure 9**).

4. Discussion and Conclusion

Before this study, only limited data were available on the vertical structure of the water column in the Gulf of

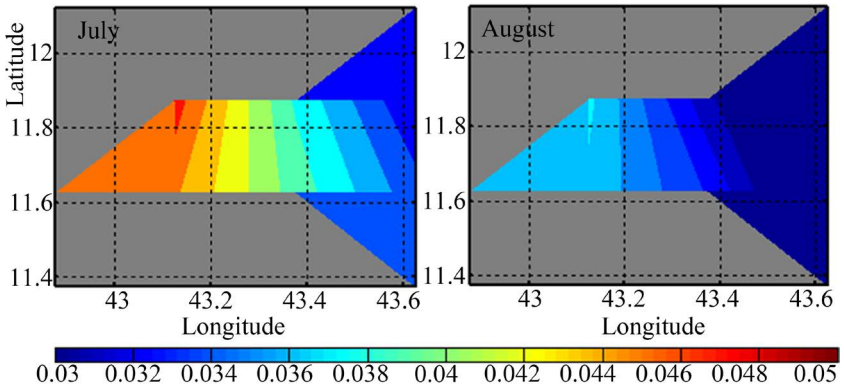

Figure 10. Wind stress field during July (left) and August (right) in the Gulf of Tadjourah. Note intensified wind stress at the extreme west of the gulf. This trend persists during August but is less accentuated.

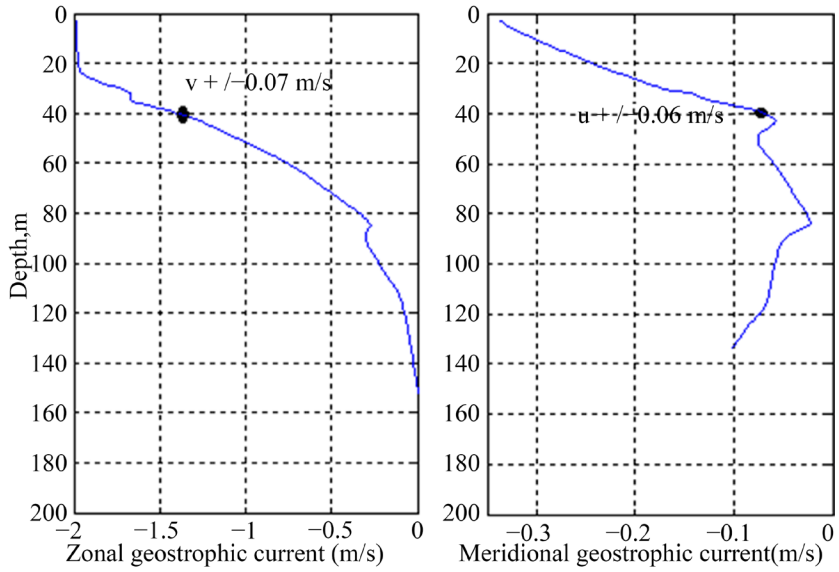

Figure 11. Zonal and meriodional geostrophic velocity during July-August.

Tadjourah. In this work, thermohaline and biogeochemical properties of the upper layer (0 - 200 m) were studied using new hydrographic data from three investigations carried out during particular months: July-August (summer), September 2013 (transitional period) and February 2014 (middle of winter when the sea surface temperature is the lowest).

During July-August, vertical temperature profiles revealed a stratified structure of three main layers. This structure was also observed for salinity, CHL-*a* concentration and DO profiles. The first striking characteristic of the water column during summer is its spatial variability. The thermally more or less homogeneous area (mixed layer) extends from the surface to about 30 m depth, but varies from one station to another. This variation is statistically significant because the difference of the mixed layer depth (H_T or MLD) between some stations exceeds the *depth uncertainty* (±0.003 - 0.004 m) *and* the standard error estimated from a set of 16 temperature profiles $\left(\varepsilon = \frac{\sigma}{\sqrt{N}} \approx 2.3 \text{ m}\right)$.

The spatial differences between stations indicate the heterogeneity of the mixed layer and appear to be related essentially to wind stress, which in turn is influenced by the topographical features. Indeed, the southwest winds which predominate during July-August affect the western part of the gulf more significantly than the eastern part (see **Figure 11**). This would induce eastward movement of surface water subsequently causing a thinning of the

mixed layer in the west of the gulf. It is proposed that the eastward displacement of surface waters by the SW monsoon winds is compensated by westward advection of near-surface waters and upwelling in the extreme west.

Evidence of Near Surface Westward Advection and Upwelling in the Extreme West of the Gulf

The measured current at station E2 during July-August clearly indicates westward inflow, which is increased at station E2 (maximum velocity at 50 m depth). This current becomes weaker in the south (St. C1) and in the west (St. W1). So, thermocline water is injected into the gulf by advection in the northeastern part and then propagates toward the west. In the extreme west, upwelling brings the thermocline water to the surface where it mixes with the surface water. This is well illustrated by the East-West temperature and DO sections (**Figure 7**). In the east, isotherm 29˚C is quasi-vertical; this indicates the presence of advected and thermally homogenous water. In contrast, isotherms 27˚C and 28˚C are parallel and deeper in the east, but become inclined and close to the surface in the west. Near surface water with low DO at the extreme west is also a good indication of the upwelling and the mixing of deep water with the surface water (**Figure 7(b)**).

In addition, the thermocline water is characterized by high salinity (S > 38). The East-West salinity section shows that the saltier layer extends from the east to the west (**Figure 7(c)**). This is in agreement with the explanation proposed above and confirms a lateral intrusion of high salinity water from the east. The maximum CHL-*a* concentration in the west is likewise consistent with the weakening of the mixed layer and the vertical supplying of nutrients from deep water. The patch of high CHL-*a* concentration (see East-West section of the CHL-*a*) is an indicator of biological activity enhanced by the upwelled nutrient rich water in the west of the gulf.

During September, the mixed layer deepens slightly and becomes thermally more homogeneous but the stratification into three main layers persists. September is a transition period during which winds are very weak. Hence, the increase of temperature and salinity could be related to solar heating of the surface water. In contrast, the deepening of the mixed layer and the thermocline in February is caused by NE monsoon winds which induce surface water flow toward the GOT (convergence). As the NE wind is cold, it cools down the surface water and induces deep convective mixing.

The monsoon winds and their seasonal reversal are the most important forces which govern surface circulation in the west of the Gulf of Aden [13]-[15]. The SW monsoon induces eastward movement of surface water, enhances upwelling in the western part through deep eddies and Ekman pumping [16]-[18]. However, in the GOT, the effects of the SW monsoon winds, particularly the induced upwelling occurs preferentially at the extreme west and southeast part of the gulf. This appears to be governed essentially by topography. It is suggested that these in turn influence SST and CHL-*a* variation at the surface of the GOT. As shown in **Figure 4**, temperature varies between stations at the surface. They range from 27.5˚C in the west (St. W1) to 29.71˚C in the east (St. E4) of the GOT. Note that the east-west temperature difference is 2.21˚C and is consistent with what was found in our previous work based on satellite data [3]. Temperatures remain lower in the western part of the gulf where the thermocline is shallower. The observed SST drop and the CHL-*a* peak during July-August are due to upwelling in the extreme west. This seems enhanced by the topographical features of the GOT. The basin is bowl-shaped and elongated along the east-west axis and more shallow in the west (**Figure 1**). This strengthens the wind stress on the western side where a significant volume of surface water is moved (**Figure 11**).

Moreover, because of the presence of islands (Musha & Maskali) at the entrance of the gulf, the near surface water containing thermocline enters the Gulf predominantly at the northeastern part, between stations E2 and E4, where the strongest westward current was observed. The high salinity of the near surface water is possibly due to the mixing with Red Sea water before entering into the GOT. This interpretation is consistent with Obura's observations [7] who reported that at the end of summer, the thermocline water that cannot pass the threshold of the Bab-el Mandeb Strait, pours onto the northeast coast of Djibouti. **Figure 12** summarizes the preeminent processes which govern surface and sub-surface structure of the upper layer in the GOT.

Acknowledgements

This work was supported financially by the "Centre d'Etude et de Recherche de Djibouti (CERD)". We are grateful to Dr Mohamed JALLUDIN and to Dr Abdulrahman DAHER for their support and encouragement

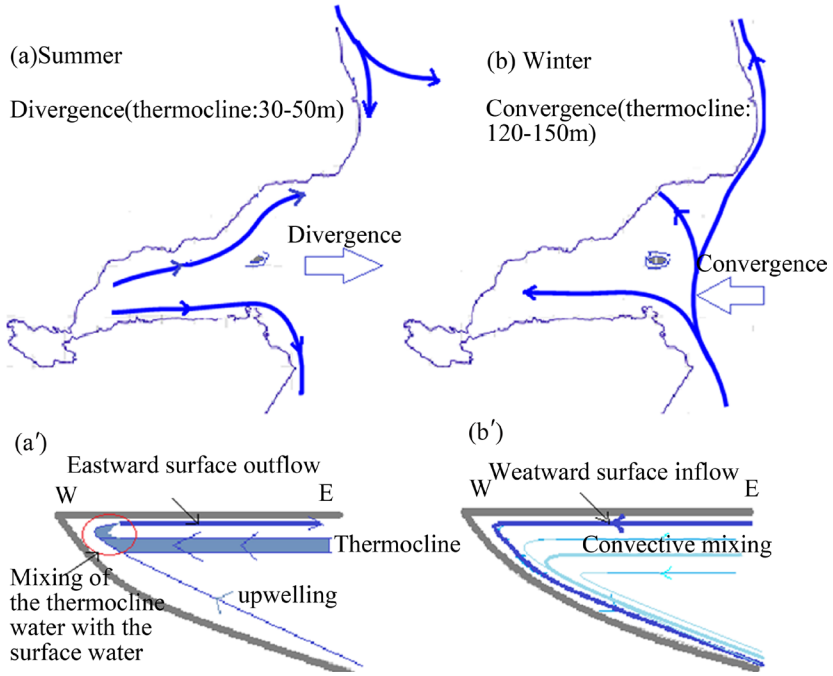

Figure 12. Diagram showing surface and sub-surface circulation patterns deduced from surface wind direction, Ekman derived currents and temperature sections.

during this study. Many thanks to the Djiboutian coast guard for their logistic support during the sampling campaign. We acknowledge LEMAR (Marine Environmental Sciences Laboratory) and LPO (*Ocean Physics* Laboratory) and "Université de Djibouti" for technical support and for providing measuring instruments. We also thank all those who contributed to this work, in particular Dr Sharon WOOLSEY for helpful comments.

References

[1] Bosworth, W., Huchon, P. and McClay, K. (2005) The Red Sea and Gulf of Aden Basins. *Journal of African Earth Sciences*, **43**, 334-378. http://dx.doi.org/10.1016/j.jafrearsci.2005.07.020

[2] Bonatti, E., Cipriani, A. and Lupi, L. (2015) The Red Sea: Birth of Ocean. In: *The Red Sea*: *The Formation, Morphology, Oceanography and Environment of a Young Ocean Basin*, Springer-Verlag, Berlin Heidelberg, 29-44. http://dx.doi.org/10.1007/978-3-662-45201-1_2

[3] Moussa Omar, Y., Memery, L. and Carton, X. (2015) Statistical Analysis of Sea Surface Temperature and Chlorophyll-*a* Concentration Patterns in the Gulf of Tadjourah (Djibouti). *Journal of Marine Sciences*: *Research and Development*, **6**, 186.

[4] Myklevoll, S. (1982) A Pelagic Fish Survey in the EEZ of the Republic of Djibouti (March 1981): Bergen, Norway, Institute of Marine Research, Reports on Surveys with the R/V DR. FRIDTJOF NANSEN, 18 p.

[5] Robineau, D. and Rose, J.-M. (1982) Le dugong [*Dugong dugon* (Müller, 1776) Sirenia, Dugongidae] en République de Djibouti. *Biological Conservation*, **24**, 233-238. http://dx.doi.org/10.1016/0006-3207(82)90060-X

[6] Bouhlel, M. (1988) Poissons de Djibouti. RDA International, Inc., Placerville, CA, Etats-Unis, 416 p.

[7] Obura, D. (1999) Evaluation Marine et Côtière, République de Djibouti. Rapport Technique no. 4 sur la Biodiversité. Projet PNUD/UICN Biodiversité de Djibouti. Direction de l'Environnement, Djibouti et UICN, Nairobi, 84 p.

[8] Chu, P.C. and Fan, C.W. (2010) Optimal Linear Fitting for Objective Determination of Ocean Mixed Layer Depth from Glider Profiles. *Journal of Atmospheric and Oceanic Technology*, Vol., pp. http://dx.doi.org/10.1175/2010JTECHO804.1

[9] Chu, P.C. and Fan, C.W. (2011) Determination of Ocean Mixed Layer Depth from Profile Data. *Proceedings on* 15*th Symposium on Integrated Observing and Assimilation Systems for the Atmosphere, Oceans and Land Surface* (*IOAS-AOLS*), American Meteorological Society, Seattle, 23-27 January 2011, 1001-1008.

[10] Brainerd, K.E. and Gregg, M.C. (1995) Surface Mixed and Mixing Layer Depths. *Deep Sea Research Part I*: *Oceano-*

graphic Research Papers, **42**, 1521-1543. http://dx.doi.org/10.1016/0967-0637(95)00068-H

[11] Lorbacher, K., Dommenget, D., Niiler, P.P. and Kohl, A. (2006) Ocean Mixed Layer Depth: Subsurface Proxy of Ocean-Atmosphere Variability. J. Geophys. Res., 11. http://dx.doi.org/10.1029/2003jc002157

[12] Pickard, G.L., and W.J. Emery. (1990) Descriptive Physical Oceanography: An Introduction. 5th Edition, Pergamon Press, New York, 320 p.

[13] Smith, S.L., Codispoti, L.A., Morrison, J.M. and Barber, R.T. (1998) The 1994-1996 Arabian Sea Expedition: An Integrated, Interdisciplinary Investigation of the Response of the Northwestern Indian Ocean to Monsoonal Forcing. *Deep-Sea Research*, **45**, 1905-1915.

[14] Aiki, H., Takahashi, K. and Yamagata, T. (2006) The Red Sea Outflow Regulated by the Indian Monsoon. *Continental Shelf Research*, **26**, 1448-1468. http://dx.doi.org/10.1016/j.csr.2006.02.017

[15] Swallow, J.C. (1984) Some Aspects of the Physical Oceanography of the Indian Ocean. *Deep Sea Research*, **31**, 639-650. http://dx.doi.org/10.1016/0198-0149(84)90032-3

[16] Luther, M.E. and O'Brien, J.J. (1985) A Model of the Seasonal Circulation in the Arabian Sea Forced by Observed Winds. *Progress in Oceanography*, **14**, 353-385. http://dx.doi.org/10.1016/0079-6611(85)90017-5

[17] Bauer, S., Hitchcock, G.L. and Olson, D.B. (1991) Influence of Monsoonally-Forced Ekman Dynamics upon Surface Layer Depth and Plankton Biomass Distribution in the Arabian Sea. *Deep-Sea Research*, **38**, 531-553. http://dx.doi.org/10.1016/0198-0149(91)90062-K

[18] Bower, A.S. and Furey, H.H. (2011) Mesoscale Eddies in the Gulf of Aden and Their Impact on the Spreading of Red Sea Outflow Water. *Progress in Oceanography*, **96**, 14-39. http://dx.doi.org/10.1016/j.pocean.2011.09.003

Appendix 1: Monthly Mean for 2013 of Ekman Derived Current Superimposed to the Wind Stress for the Western Part of the Gulf of Aden and the Southern Region of the Red Sea